Relativistic Impulse Approximation & Millichaged Particle

Chen-Kai Qiao

College of Science

Chongqing University of Technology

目录

CONTENTS

Millicharged Particle (MCP)

Millicharged Particles

Charge Quantization

The electric charge of millicharge particle is not quantized. It challenges the charge quantization.

Beyond the Standard Model

Millicharge particle (MCP) is predicted by theories beyond the Standard Model
It is connected with the following issues:

- Dark Matter
- Nutrino Physics
- Astroparticle Physics & Cosmology

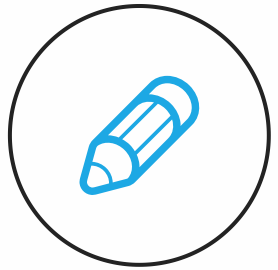

Tiny Electromagetic Interaction

Millicharge particle (MCP) has tiny electric charge (usually less than 10^{-5} e).
It could interact with Standard Model charged particles via electromagnetic interaction.

Millicharged Particle : Mechanism

Introducing additional hidden U(1) gauge group

$$\begin{aligned}\mathcal{L} &= \mathcal{L}_0 + \mathcal{L}_1 \\ &= -\frac{1}{4}F_{\mu\nu}F^{\mu\nu} - \frac{1}{4}V_{\mu\nu}V^{\mu\nu} - \frac{\kappa}{2}F_{\mu\nu}V^{\mu\nu} + J^B_\mu B^\mu + J^C_\mu C^\mu\end{aligned}$$

Phys. Rev. D 75, 115001 (2007)

$$B^\mu = \frac{1}{\sqrt{1-\kappa^2}}A^\mu$$

$$C^\mu = -\frac{\kappa}{\sqrt{1-\kappa^2}}A^\mu + \tilde{A}^\mu$$

SM Sector

Hidden Sector

$$\begin{aligned}\mathcal{L}_1 &= J^B_\mu B^\mu + J^C_\mu C^\mu \\ &= \left[\frac{1}{\sqrt{1-\kappa^2}}J^B_\mu - \frac{\kappa}{\sqrt{1-\kappa^2}}J^C_\mu\right]A^\mu + J^C_\mu \tilde{A}^\mu\end{aligned}$$

SM fermion

MCP

Photon

Dark Photon

millicharge

$$q_\chi \equiv \delta_\chi e = -\frac{\kappa}{\sqrt{1-\kappa^2}}g_h$$

$$\delta_\chi = -\frac{\kappa}{\sqrt{1-\kappa^2}}\frac{g_h}{e}$$

Millicharged Particle : Mechanism

Introducing Right-handed Massive Fermion

$$\begin{aligned}\mathcal{L} &= \mathcal{L}_0 + \mathcal{L}_1 \\ &= -\frac{1}{4}F_{\mu\nu}F^{\mu\nu} - \bar{\chi}(ic\hbar\gamma^\mu\partial_\mu - m_\chi c^2)\chi + \delta_\chi e\bar{\chi}\gamma_\mu B^\mu\chi\end{aligned}$$

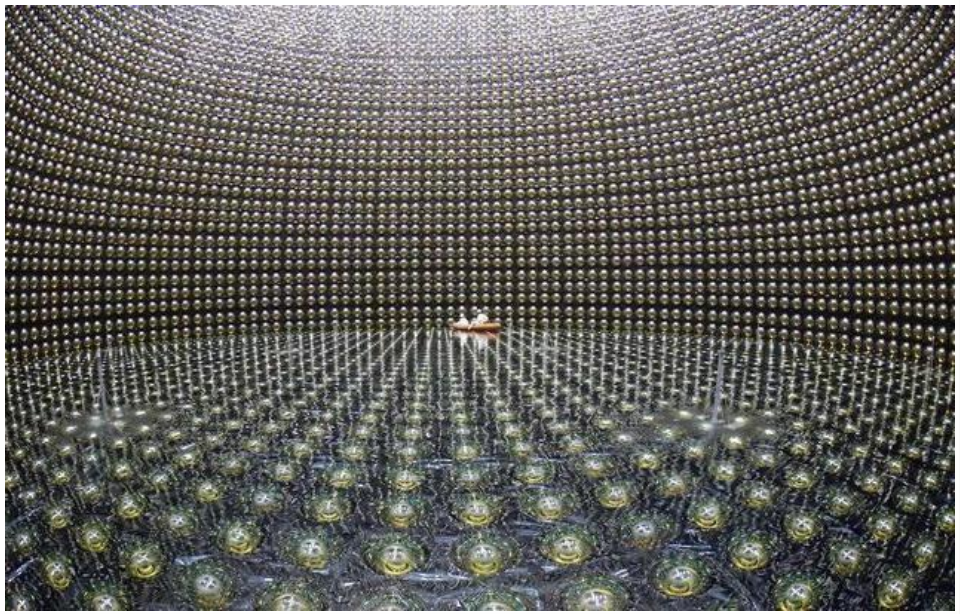

- It may Connects with SU(2) right-handed neutrino.
- (Millicharged Neutrino)

millicharge

$$q_\chi = \delta_\chi e.$$

N. Vinyoles and H. Vogel, J. Cosmol. Astropart. Phys. 03(2016) 002

Parameter Space of Milicharged Dark Matter Particle

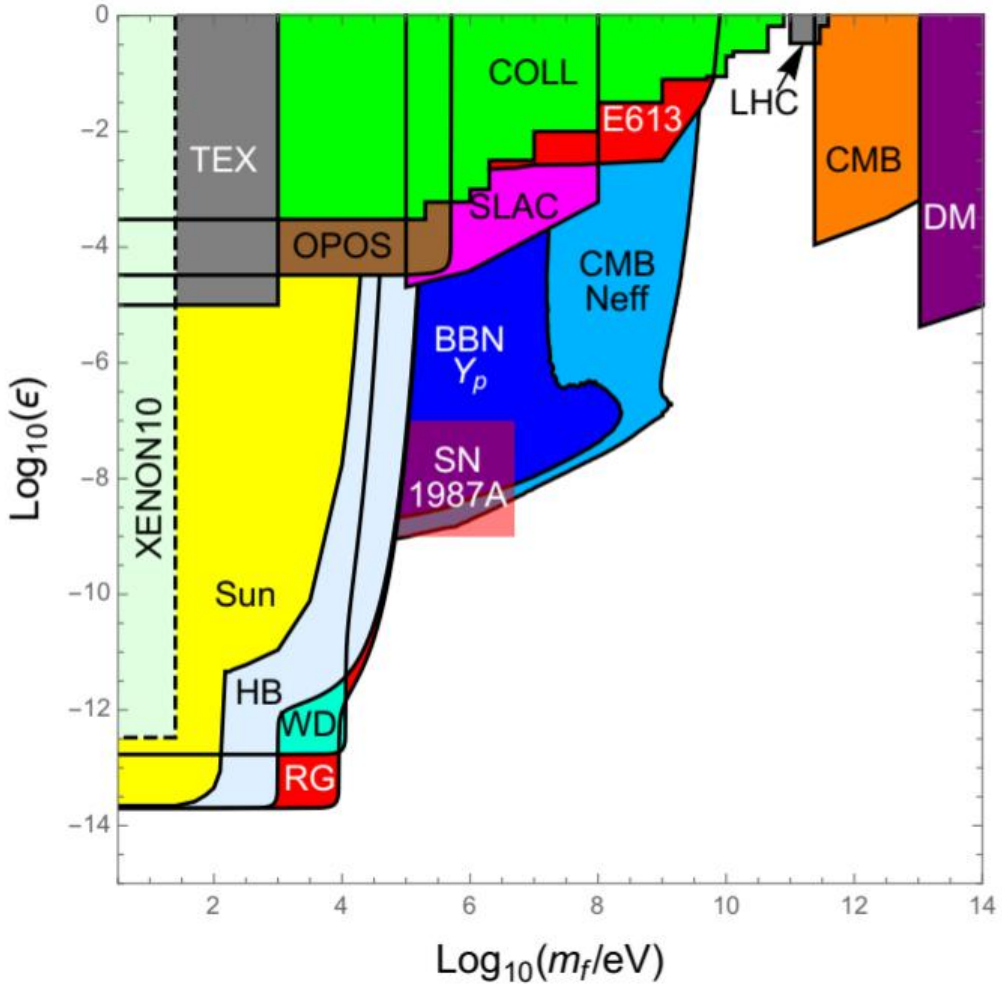

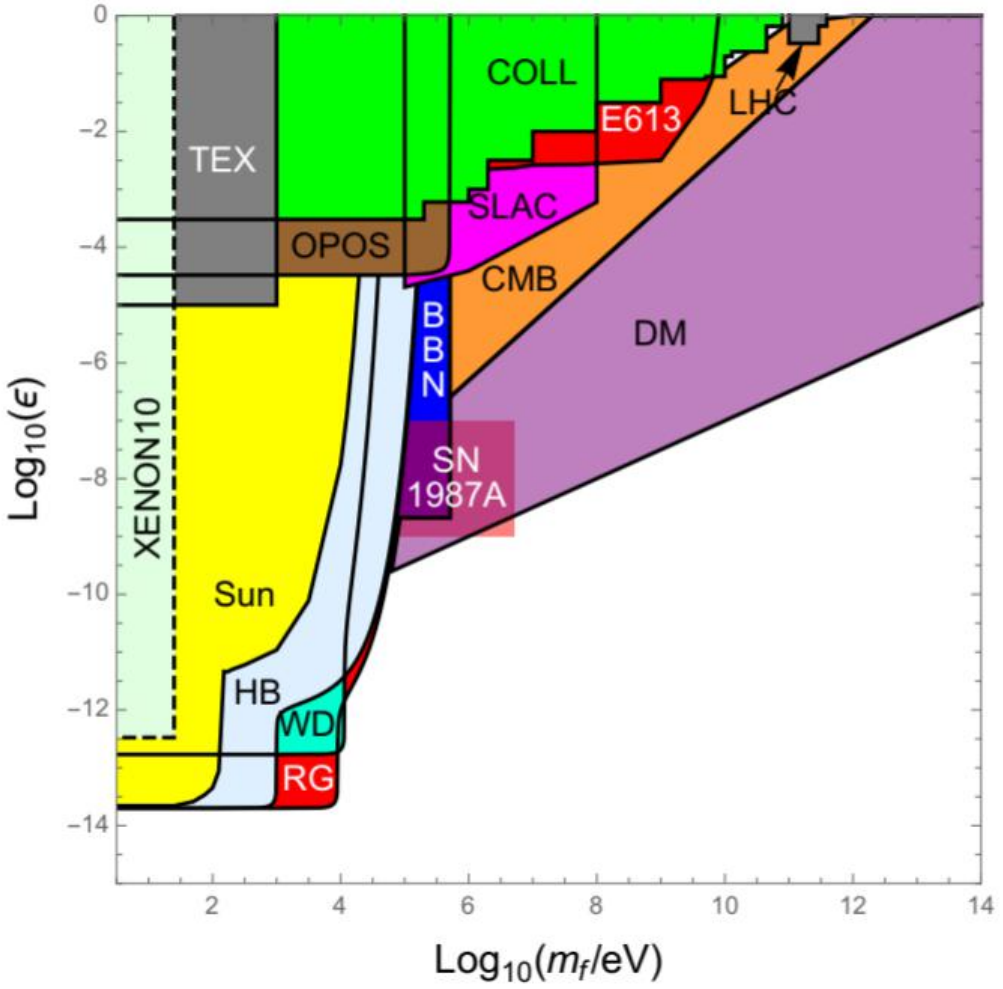

N. Vinyoles and H. Vogel, J. Cosmol. Astropart. Phys. 03(2016) 002

Experimental Constraint on Neutrino Millicharge

TABLE V. Approximate limits for different neutrino effective charges. The limits on q_ν apply to all flavors.

Limit	Method	Reference
$\lvert q_{\nu_\tau}\rvert \lesssim 3 \times 10^{-4} e$	SLAC e^- beam dump	Davidson, Campbell, and Bailey (1991)
$\lvert q_{\nu_\tau}\rvert \lesssim 4 \times 10^{-4} e$	BEBC beam dump	Babu, Gould, and Rothstein (1994)
$\lvert q_\nu\rvert \lesssim 6 \times 10^{-14} e$	Solar cooling (plasmon decay)	Raffelt (1999a)
$\lvert q_\nu\rvert \lesssim 2 \times 10^{-14} e$	Red giant cooling (plasmon decay)	Raffelt (1999a)
$\lvert q_{\nu_e}\rvert \lesssim 3 \times 10^{-21} e$	Neutrality of matter	Raffelt (1999a)
$\lvert q_{\nu_e}\rvert \lesssim 3.7 \times 10^{-12} e$	Nuclear reactor	Gninenko, Krasnikov, and Rubbia (2007)
$\lvert q_{\nu_e}\rvert \lesssim 1.5 \times 10^{-12} e$	Nuclear reactor	Studenikin (2014)

Experimental Constraint on Neutrino Charge Radius

TABLE VI. Experimental limits for the electron neutrino charge radius.

Method	Experiment	Limit (cm^2)	C.L.	Reference
Reactor $\bar{\nu}_e$-e^-	Krasnoyarsk	$\lvert\langle r^2_{\nu_e}\rangle\rvert < 7.3 \times 10^{-32}$	90%	Vidyakin *et al.* (1992)
	TEXONO	$-4.2 \times 10^{-32} < \langle r^2_{\nu_e}\rangle < 6.6 \times 10^{-32}$	90%	Deniz *et al.* (2010)[a]
Accelerator ν_e-e^-	LAMPF	$-7.12 \times 10^{-32} < \langle r^2_{\nu_e}\rangle < 10.88 \times 10^{-32}$	90%	Allen *et al.* (1993)[a]
	LSND	$-5.94 \times 10^{-32} < \langle r^2_{\nu_e}\rangle < 8.28 \times 10^{-32}$	90%	Auerbach *et al.* (2001)[a]
Accelerator ν_μ-e^-	BNL-E734	$-4.22 \times 10^{-32} < \langle r^2_{\nu_\mu}\rangle < 0.48 \times 10^{-32}$	90%	Ahrens *et al.* (1990)[a]
	CHARM-II	$\lvert\langle r^2_{\nu_\mu}\rangle\rvert < 1.2 \times 10^{-32}$	90%	Vilain *et al.* (1995)[a]

[a]The published limits are half, because they use a convention which differs by a factor of 2 [see also Hirsch, Nardi, and Restrepo (2003)].

Rev. Mod. Phys. 87(02), 531-591 (2015)

Relativistic Impulse Approximation

Relativistic Impulse Approximation

RIA is a method developed in 1970s-1980s to dual with the manybody electromagnetic interactions in atomic and molecular physics

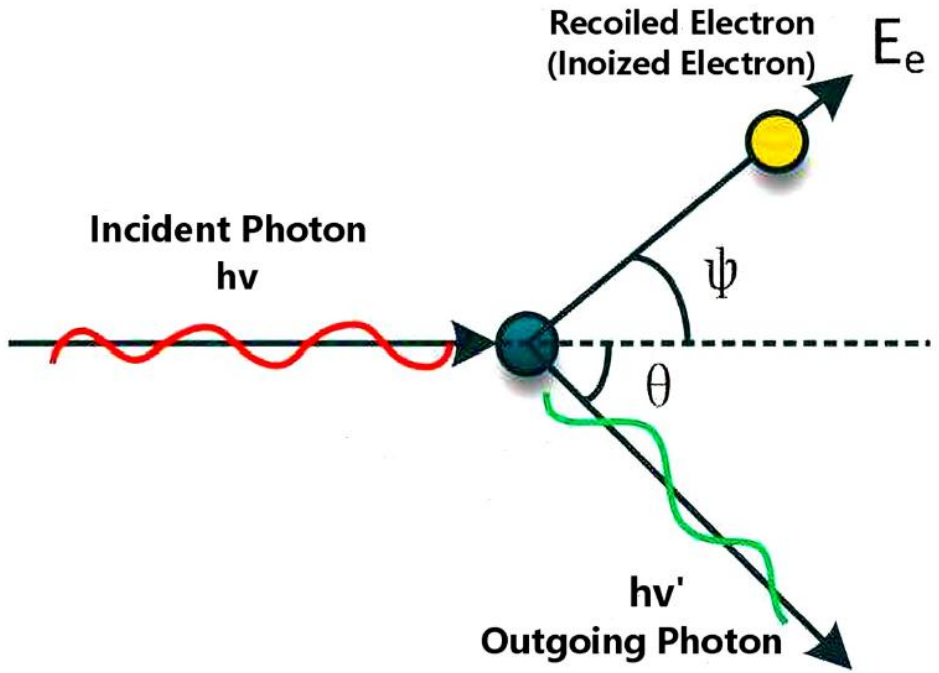

Compton Scattering

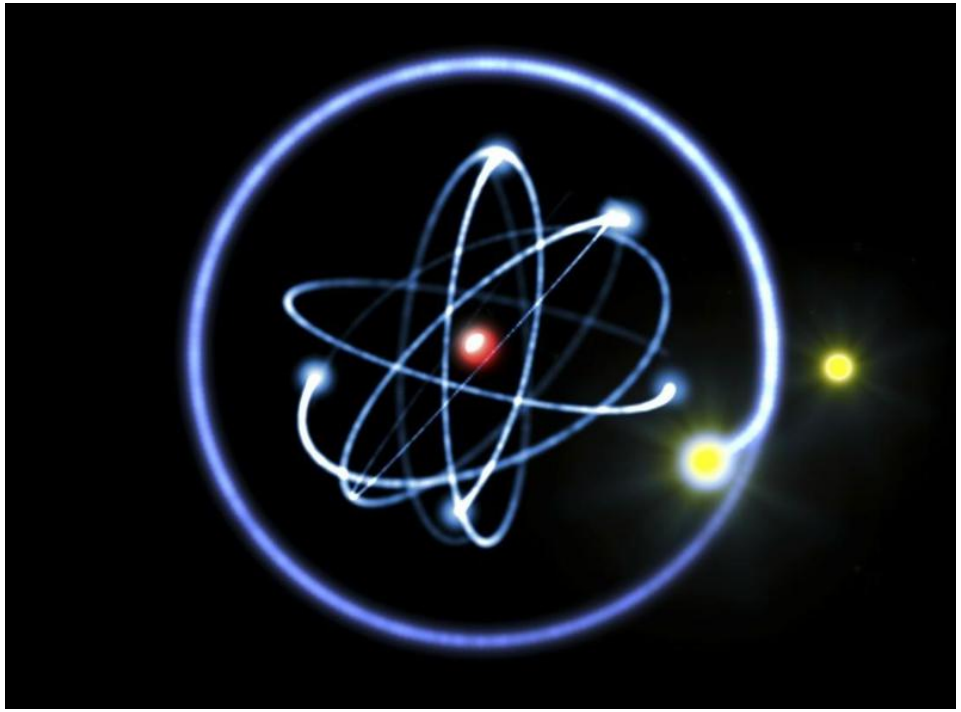

Electron Impact / Electron-Ion collision

Relativistic Impulse Approximation

Free Electron Approximation

- Free electron is usually viewed as momentum eigenstate.
- It scattered with incident charged particles independently.

Impulse Approximation

- Bound electron in atoms has a momentum distribution when moving alound atomic nuclei.
- In the scattering process, electron scatters with incident particles very rapidly, like an impulse acting on electron. This scattering process is too quick to be disturbed by other electrons.
- Assumption: Monentum eigenstate electron scattered with incident charged particles independently. Interference terms between different momentum eigenstates are neglected

Impulse Approximation

- **Each monentum eigenstate electron scattered with incident charged particles independently. Interference terms between different momentum eigenstates are neglected**

$$\left(\frac{d^2\sigma}{d\omega_f d\Omega_f}\right)_{\mathrm{RIA}} = \int \left(\frac{d^2\sigma}{d\omega_f d\Omega_f}\right)^{\mathrm{QED}}_{p_i=p} \rho(\boldsymbol{p}) d^3p \quad \rightarrow \quad \left(\frac{d^2\sigma}{d\omega_f d\Omega_f}\right)_{\mathrm{RIA}} = C \cdot J(p_z)$$

approximation

Scattering Probability (momentum eigenstate electron & incident particle)

Electron momentum distribution

Compton Profile

$$J(p_z) \equiv \int \rho(\boldsymbol{p}) dp_x dp_y$$

Basic Property of RIA

$$\left(\frac{d^2\sigma}{d\omega_f d\Omega_f}\right)_{\mathrm{RIA}} \propto J(p_z) \equiv \int \rho(\boldsymbol{p}) dp_x dp_y$$

RIA in Compton Scattering

Basic Sarting Point

$$\left(\frac{d^2\sigma}{d\omega_f d\Omega_f}\right)_{\mathrm{RIA}} = \frac{r_0^2 m_e^2 c^4}{2}\frac{\omega_f}{\omega_i}\iiint d^3p_i \rho(\boldsymbol{p}_i)\frac{X(K_i,K_f)}{E_i E_f}\delta(E_i+\omega_i-E_f-\omega_f)$$

$$\begin{aligned} X(K_i,K_f) &\approx \overline{X}(\overline{K}_i(p_z),\overline{K}_f(p_z)) \\ &= \frac{K_i(p_z)}{K_f(p_z)}+\frac{K_f(p_z)}{K_i(p_z)}+2m_e^2c^2\left[\frac{1}{K_i(p_z)}-\frac{1}{K_f(p_z)}\right] \\ &\quad +m_e^4c^4\left[\frac{1}{K_i(p_z)}-\frac{1}{K_f(p_z)}\right]^2 \end{aligned}$$

$$X(K_i,K_f) \approx X_{\mathrm{KN}} = \frac{\omega_i}{\omega_f}+\frac{\omega_f}{\omega_i}-\sin^2\theta$$

R.Ribberfors (1975-1982)
Making simpified approximation for X

$$\left(\frac{d^2\sigma}{d\omega_f d\Omega_f}\right)_{\mathrm{RIA}} = Y^{\mathrm{RIA}} J(p_z)$$

$$\left(\frac{d\sigma}{d\Omega_f}\right)_{\mathrm{RIA}} = \left(\frac{d\sigma}{d\Omega}\right)_{\mathrm{FEA}} S(\omega_i,\theta)$$

$$\left(\frac{d\sigma}{dT}\right)_{\mathrm{RIA}} = \int d\Omega_f \left(\frac{d^2\sigma}{d\omega_f d\Omega_f}\right)_{\mathrm{RIA}}$$

Kinematical Factor
Indenpendent of the target materials.

Compton Profile
Closely related to the properties of target materials.

FEA Results

Scattering Function

Compton Profile

Basic Property of RIA

$$\left(\frac{d^2\sigma}{d\omega_f d\Omega_f}\right)_{\mathrm{RIA}} \propto J(p_z) \equiv \int \rho(\boldsymbol{p}) dp_x dp_y$$

Compton Profile

$$J(p_z) \equiv \iint \rho(\boldsymbol{p}_i) dp_x dp_y$$

$$\rho(p) = \sum_{a=1}^{Z} |\phi_a(\boldsymbol{p})|^2$$

Compton Profile is connected with the electron momentum density in atoms and molecular systems

It is closely related to the elecronic structures and properties of target materials.

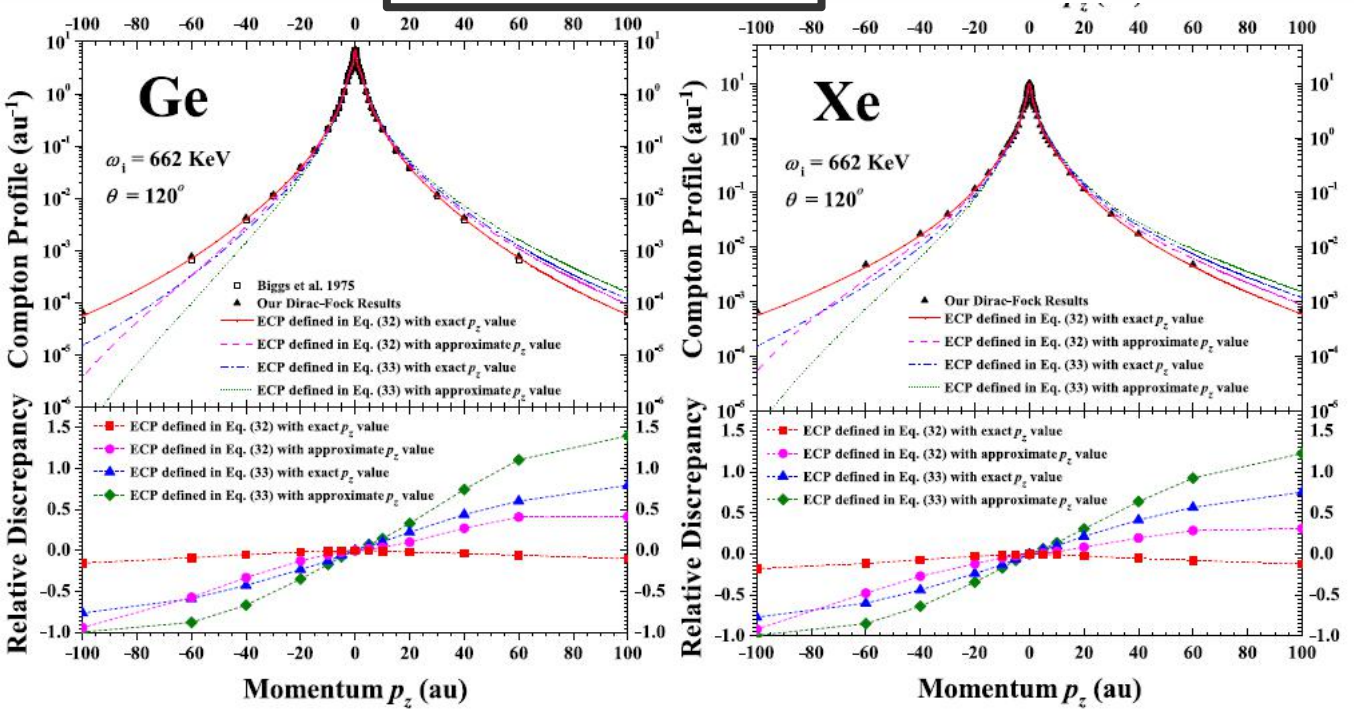

Qiao et al.
Journal of Physics B: Atomic and Molecular Physics 53, 075002 (2020)
arXiv: 1902.02301[physics.atom-ph]

RIA in the Compton Scattering: Results

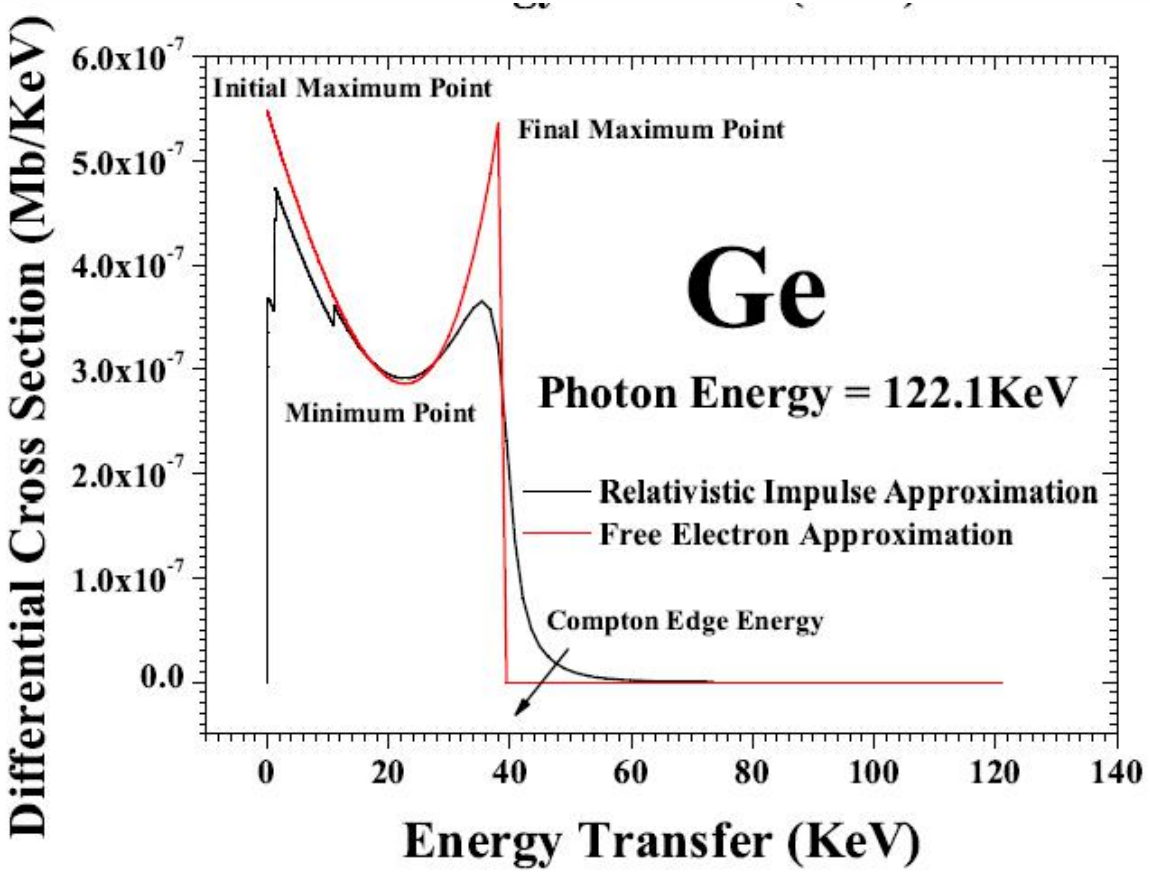

Qiao et al.
Compton Scattering Energy Spectrums for Si and Ge Systems
arXiv: 1907.09868[physics.atom-ph]
Journal of Physics G: Nuclear and Particle Physics 47, 045202 (2020)

Differential Cross Section

$$\left(\frac{d^2\sigma}{d\omega_f d\Omega_f}\right)_{\mathrm{RIA}} = \frac{r_0^2}{2}\frac{m_e}{q}\frac{m_e c^2}{E(p_z)}\frac{\omega_f}{\omega_i}\overline{X}(p_z)J(p_z)$$

Compton Profile

RIA in the Atomic Ionization induced by MCP

RIA in the Atomic Ionization induced by MCP

Starting Point

$$\left(\frac{d^2\sigma}{dE'_\chi d\Omega_f}\right)_{\text{RIA}} = \frac{r_0^2 m^2 c^4}{2}\frac{E'_\chi}{E_\chi}\iiint d^3p_i \rho(\boldsymbol{p}_i)\frac{X}{E_i E_f}\delta(E_i + E_\chi - E_f - E'_\chi)$$

Atomic Compton Scattering

$$\gamma + A \to \gamma' + A^+ + e^-$$

$$X = X(K_i, K_f) = \frac{K_i}{K_f} + \frac{K_f}{K_i} + 2m^2c^2\left(\frac{1}{K_i} - \frac{1}{K_f}\right) + m^4c^4\left(\frac{1}{K_i} - \frac{1}{K_f}\right)^2$$

For atomic ionition process induced by MCP, the scattering probabilities can be obtained similar to the Rutherford scattering

Rutherford scattering

$$e^- p^+ \to e^- p^+$$

$$\frac{1}{4}\sum_{\text{spins}}|\mathcal{M}|^2 = \frac{2e^4}{t^2}\left[u^2 + s^2 + 4t(m_e^2 + m_p^2) - 2(m_e^2 + m_p^2)^2\right].$$

Atomic Ionization process induced by MCP

$$\chi + A \to \chi + A^+ + e^-$$

$$X = \delta_\chi^2 \frac{u^2 + s^2 + 4t(m_e^2c^4 + m_\chi^2c^4) - 2(m_e^2c^4 + m_\chi^2c^4)^2}{t^2}$$

Differential Cross Section

Starting Point

$$\left(\frac{d^2\sigma}{dE'_\chi d\Omega_f}\right)_{\text{RIA}} = \frac{r_0^2 m^2 c^4}{2}\frac{E'_\chi}{E_\chi}\iiint d^3p_i \rho(\boldsymbol{p}_i)\frac{X}{E_i E_f}\delta(E_i + E_\chi - E_f - E'_\chi)$$

$$X = \delta_\chi^2 \frac{u^2 + s^2 + 4t(m_e^2c^4 + m_\chi^2 c^4) - 2(m_e^2c^4 + m_\chi^2c^4)^2}{t^2}$$

$$X \approx \overline{X}(\bar{s}(p_z), \bar{t}(p_z), \bar{u}(p_z))$$
$$= \delta_\chi^2 \frac{\bar{u}(p_z)^2 + \bar{s}(p_z)^2 + 4\bar{t}(p_z)(m_e^2c^4 + m_\chi^2c^4) - 2(m_e^2c^4 + m_\chi^2c^4)^2}{\bar{t}(p_z)^2}$$

$$\bar{s}(p_z) = m_e^2c^4 + m_\chi^2c^4 + 2\left[E(p_z)E_\chi + \frac{k_i(k_i - k_f\cos\theta)p_z c^2}{q}\right]$$
$$\bar{t}(p_z) = t = 2m_\chi^2c^4 - 2\left(E_\chi E'_\chi - k_i k_f c^2\cos\theta\right)$$
$$\bar{u}(p_z) = m_e^2c^4 - m_\chi^2c^4 + 2\left(E_\chi E'_\chi - k_i k_f c^2\cos\theta\right)$$
$$-2\left[E(p_z)E_\chi + \frac{k_i(k_i - k_f\cos\theta)p_z c^2}{q}\right]$$

Making approximation for X

Doubly-differential Cross Section (DDCS)

$$\left(\frac{d^2\sigma}{dE'_\chi d\Omega_f}\right)_{\text{RIA}} = \frac{r_0^2}{2}\frac{m_e}{q}\frac{m_e c^2}{E(p_z)}\frac{E'_\chi}{E_\chi}\overline{X}(\bar{s}(p_z), \bar{t}(p_z), \bar{u}(p_z))J(p_z)$$

Kinematical Factor
Indenpendent of target materials.

Compton Profile
Closely related to the properties of target materials.

Differential Cross Section (Simplified Verion)

Starting Point

$$\left(\frac{d^2\sigma}{dE'_\chi d\Omega_f}\right)_{\text{RIA}} = \frac{r_0^2 m^2 c^4}{2}\frac{E'_\chi}{E_\chi}\iiint d^3p_i\rho(\boldsymbol{p}_i)\frac{X}{E_i E_f}\delta(E_i + E_\chi - E_f - E'_\chi)$$

$$X = \delta_\chi^2 \frac{u^2 + s^2 + 4t(m_e^2c^4 + m_\chi^2c^4) - 2(m_e^2c^4 + m_\chi^2c^4)^2}{t^2}$$

$$\begin{aligned} X &\approx X_{\text{sim}} \\ &= \delta_\chi^2 \frac{u_{\text{sim}}^2 + s_{\text{sim}}^2 + 4t_{\text{sim}}(m_e^2c^4 + m_\chi^2c^4) - 2(m_e^2c^4 + m_\chi^2c^4)^2}{t_{\text{sim}}^2} \end{aligned}$$

$$\begin{aligned} s_{\text{sim}} &= m_e^2c^4 + m_\chi^2c^4 + 2m_ec^2E_\chi \\ t_{\text{sim}} &= t = 2m_\chi^2c^4 - 2\left(E_\chi E'_\chi - k_i k_f c^2\cos\theta\right) \\ u_{\text{sim}} &= m_e^2c^4 - m_\chi^2c^4 - 2m_ec^2E_\chi + 2\left(E_\chi E'_\chi - k_i k_f c^2\cos\theta\right) \end{aligned}$$

Making approximation for X

Doubly-differential Cross Section (DDCS)

$$\left(\frac{d^2\sigma}{dE'_\chi d\Omega_f}\right)_{\text{RIA}} = \frac{r_0^2}{2}\frac{m_e}{q}\frac{E'_\chi}{E_\chi}X_{\text{sim}}J(p_z)$$

Kinematical Factor
Indenpendent of target materials.

Compton Profile
Closely related to the properties of target materials.

Differential Cross Section and Reation Event Rate

Doubly-differential Cross Section (DDCS)

$$\left(\frac{d^2\sigma}{dE'_\chi d\Omega_f}\right)_{\text{RIA}} = \frac{r_0^2}{2}\frac{m_e}{q}\frac{m_e c^2}{E(p_z)}\frac{E'_\chi}{E_\chi}\overline{X}(\overline{s}(p_z),\overline{t}(p_z),\overline{u}(p_z))J(p_z)$$

$$\left(\frac{d^2\sigma}{dE'_\chi d\Omega_f}\right)_{\text{RIA}} = \frac{r_0^2}{2}\frac{m_e}{q}\frac{E'_\chi}{E_\chi}X_{\text{sim}}J(p_z)$$

Singly-differential Cross Section (with respect to energy transfer T)

$$\left(\frac{d\sigma}{dT}\right)_{\text{RIA}} = \int d\Omega'_\chi \left(\frac{d^2\sigma}{dE'_\chi d\Omega'_\chi}\right)_{\text{RIA}}$$

Reaction Event Rate in HPGe and Xenon Detectors

$$\frac{dR}{dT} = \rho_A \int_{E_{\text{min}}}^{E_{\text{max}}} dE_\chi \frac{d\sigma}{dT}\frac{d\phi_\chi}{dE_\chi}$$

$$\frac{dR}{dT} = \rho_A \int_{E_{\text{min}}}^{E_{\text{max}}} dE_\nu \frac{d\sigma}{dT}\frac{d\phi_\nu}{dE_\nu}$$

Results, Discussions, and Prospects

Approach

Calculate Groundstate Energy and Wavefunction

Hartree-Fock Theory
Non-Relativistic Theory

Dirac-Fock Theory
Fully Relativistic Theory (Relativistic Generalization of Hartree-Fock Theory)

Multi-Configuration Dirac-Fock (MCDF)
Fully Relativistic Theory
Multi-configuration Generalization of the Dirac-Fock Theory

Advantages:
1. With atomic binding and electron correlation effects considered
2. Widely condirmed by experiments in atomic and molecular physics

Calculate Differential Cross Section and Reaction Event Rate

Free Electron Approximation
Electrons are treated as free electrons.
Atomic many-body effectes are neglected
Energy Transfer >> Atomic binding energy（11 keV for Ge）

Equvalent Photon Approximation
Visual exchange photons are treated as real photons
Wolks well in low-energy transfer and low-momentum transfer region.

Relativistic Impulse Approximation (Our Work)
Bound electron has a momentum distribution
Momentum eigenstate electron scatters with incident charged particle independently
Wolks well in the entire energy region

Millicharged Dark Matter Particle: Cross Section

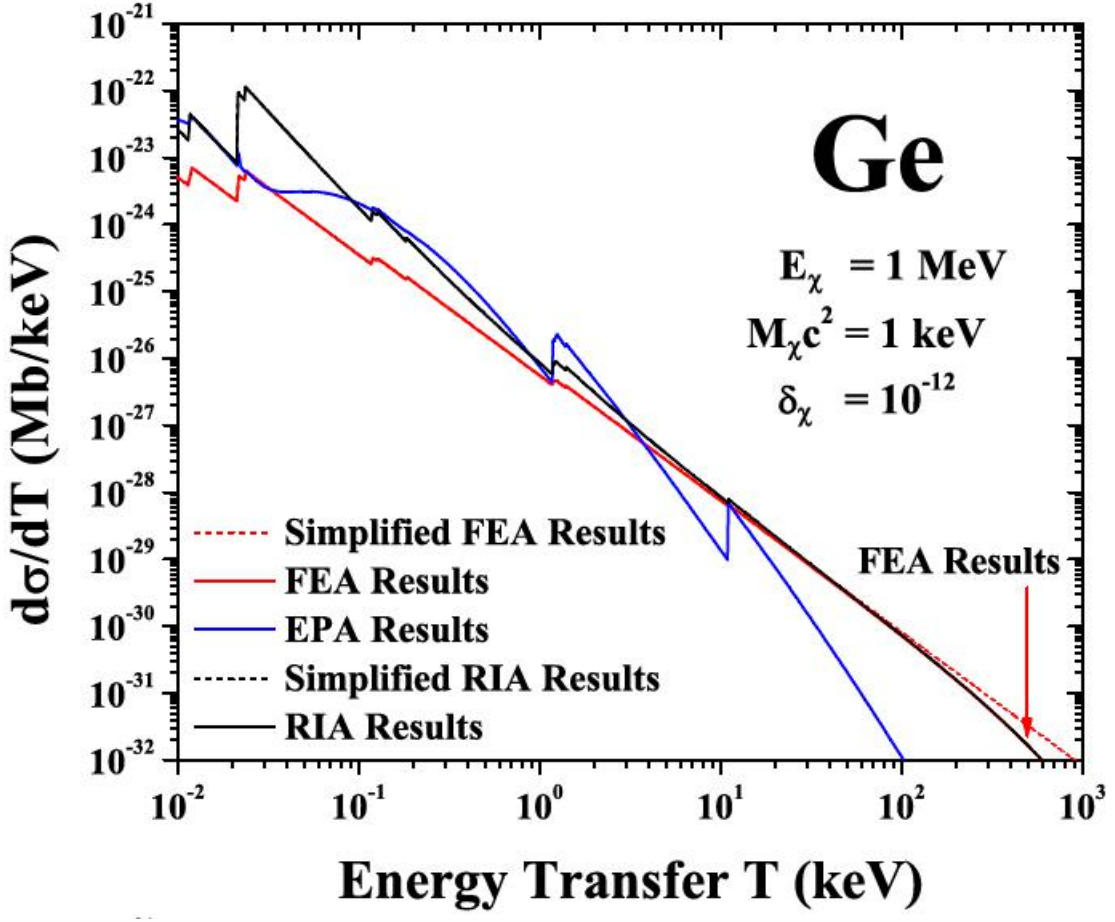

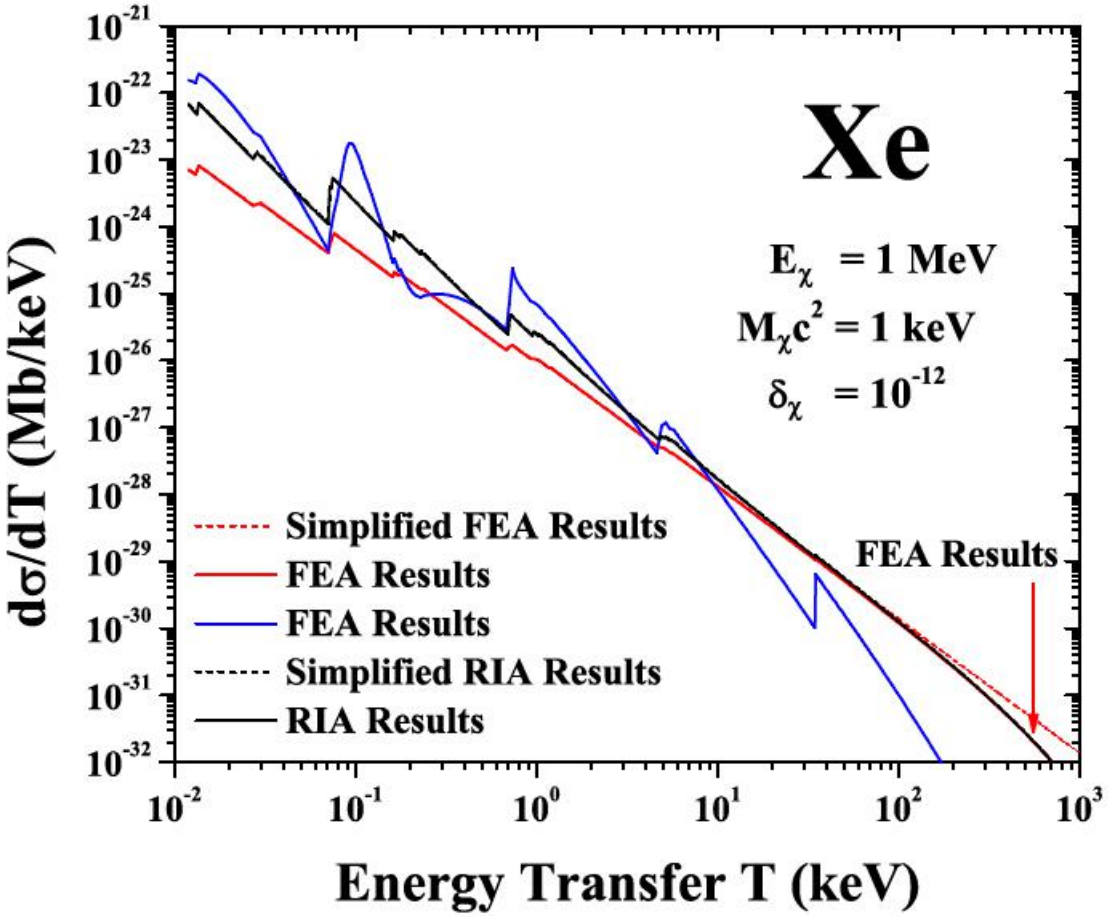

When energy transfer is sufficient large, RIA results and FEA results agree with each other

Energy Transfer >> Atomic binding energy（11.1 keV for Ge 34.5 keV for Xe）

Millicharged Dark Matter Particle

Reaction Event Rate in Detectors

$$\frac{dR}{dT} = \rho_A \int_{E_{\min}}^{E_{\max}} dE_\chi \frac{d\sigma}{dT} \frac{d\phi_\chi}{dE_\chi}$$

Assumption: millicharged dark matter particle is coming from comic rays

Flux spectrum of millicharged dark matter particle in dark comic-ray

$$\frac{d\phi_\chi}{dE_\chi} = 30\delta_\chi^{\alpha-1}\left(\frac{\mathrm{GeV}}{m_\chi c^2}\right)\left(\frac{E_\chi}{\mathrm{GeV}}\right)^{-\alpha} \mathrm{cm}^{-2}\mathrm{s}^{-1}\mathrm{GeV}^{-1}\mathrm{sr}^{-1}$$

P.-K. Hu et al., Phys. Lett. B 768, 18 (2017)

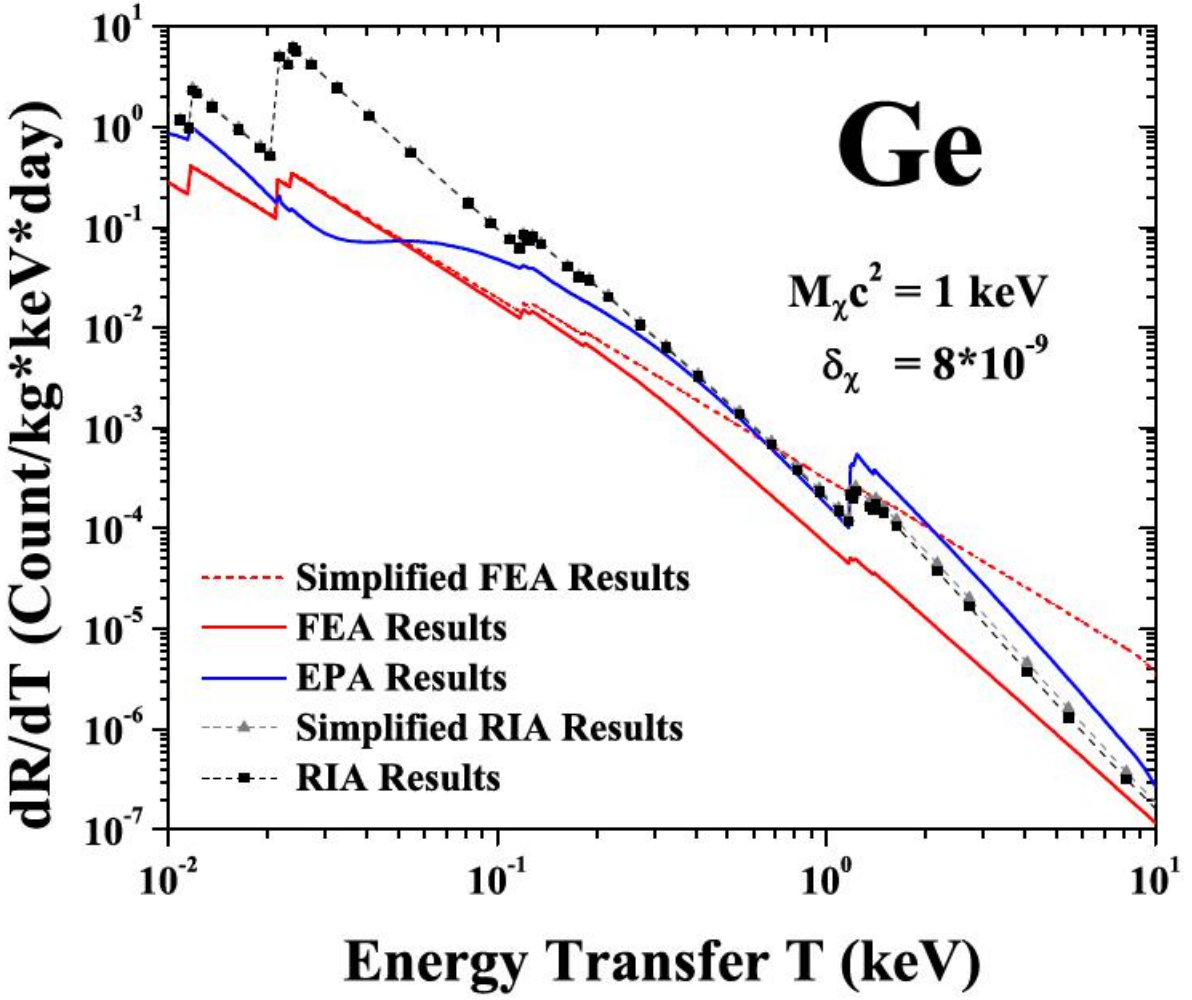

Detecting sensitivity in next generation experiments

Detecting sensitivity on millicharge (next generation HPGe based experiments)			
mass (kev)	sensitivity （FEA）	sensitivity （EPA）	sensitivity （RIA）
100	$3.7*10^{-7}$	$2.8*10^{-7}$	$2.5*10^{-7}$
10	$7.0*10^{-8}$	$5.3*10^{-8}$	$4.5*10^{-8}$
1	$1.4*10^{-8}$	$1.0*10^{-8}$	$8*10^{-9}$
0.1	$6.0*10^{-9}$	$1.9*10^{-9}$	$2*10^{-9}$
0.01	$3.2*10^{-9}$	$3.5*10^{-10}$	$1*10^{-9}$

Energy Threshold: 100eV
Experimental Background: 0.1cpkkd （count/kg·keV·day）
Reaction Event Rate > Experimental Background
---> Millicharged Dark Matter Particle can be detected

Detecting sensitivity in next generation experiments

Detecting sensitivity on millicharge (next generation Xenon based experiments)			
mass (kev)	sensitivity （FEA）	sensitivity （EPA）	sensitivity （RIA）
100	$1.3*10^{-7}$	$9.3*10^{-8}$	$1*10^{-7}$
10	$2.5*10^{-8}$	$1.8*10^{-8}$	$2*10^{-8}$
1	$5.9*10^{-9}$	$3.2*10^{-9}$	$4*10^{-9}$
0.1	$3.1*10^{-9}$	$6.0*10^{-10}$	$1.5*10^{-9}$
0.01	$1.7*10^{-9}$	$2.5*10^{-10}$	$8*10^{-10}$

Energy Threshold: 500eV
Experimental Background: 10^{-4}cpkkd （count/kg·keV·day）
Reaction Event Rate > Experimental Background
---> Millicharged Dark Matter Particle can be detected

Detecting sensitivity in next generation experiments

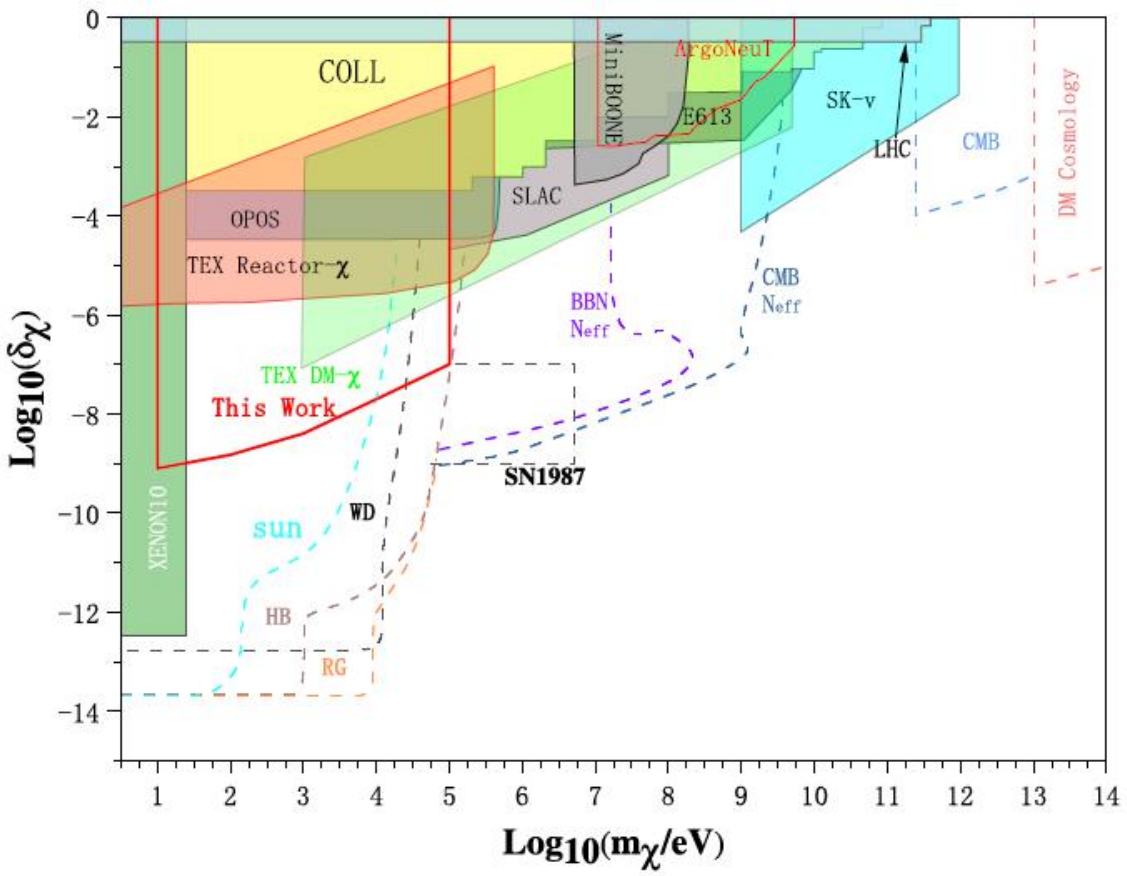

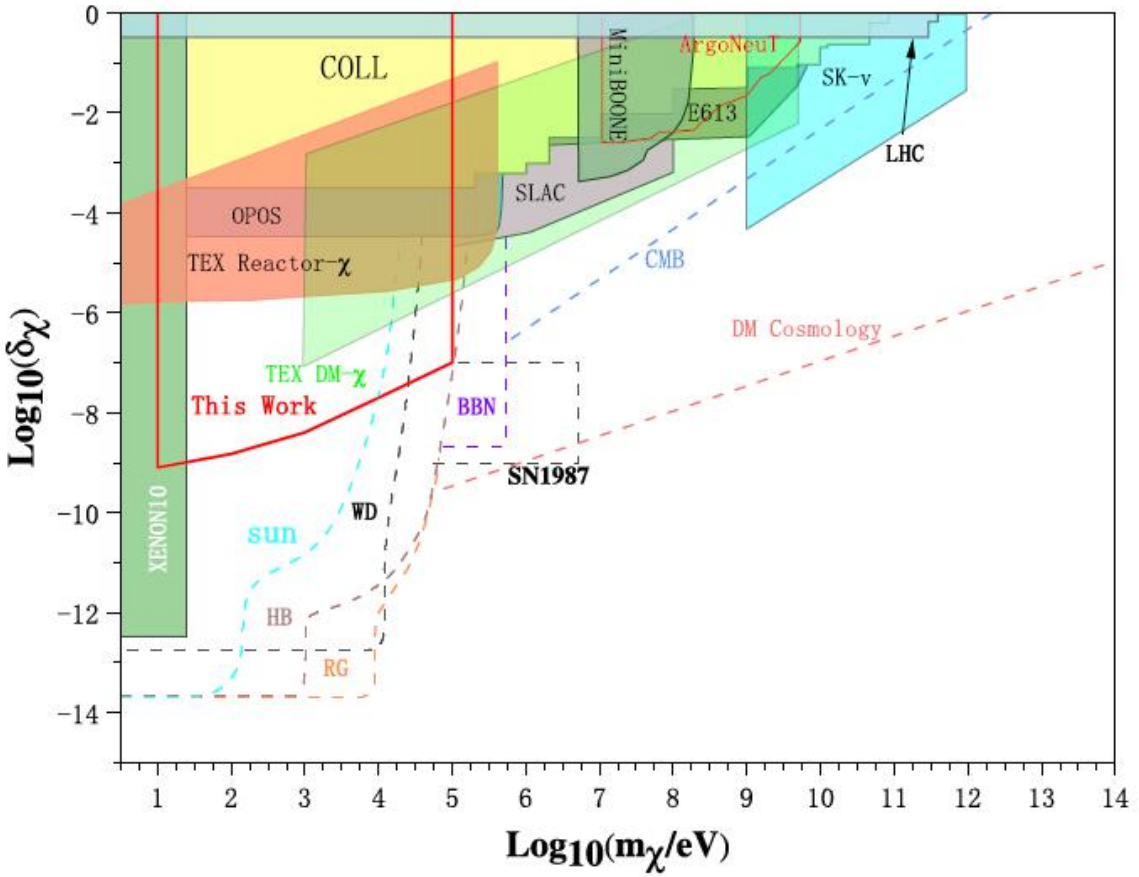

"This work" presents the detecting sensitivity of dark matter particle millicharge in next-generation Xenon based experiments calculated using RIA

Millicharged Neutrino

Reaction Event Rate in Detectors

$$\frac{dR}{dT} = \rho_A \int_{E_{\min}}^{E_{\max}} dE_\nu \frac{d\sigma}{dT} \frac{d\phi_\nu}{dE_\nu}$$

Assumption:
keV --- GeV region
millicharged neutrino is mostly coming from solar neutrinos

The pp channel and ^{7}Be channel are dominant in the solar neutrino flux spectrum.

$$\frac{d\phi_\nu}{dE_\nu} \approx \frac{d\phi_\nu^{pp}}{dE_\nu} + \frac{d\phi_\nu^{\mathrm{Be}}}{dE_\nu}$$

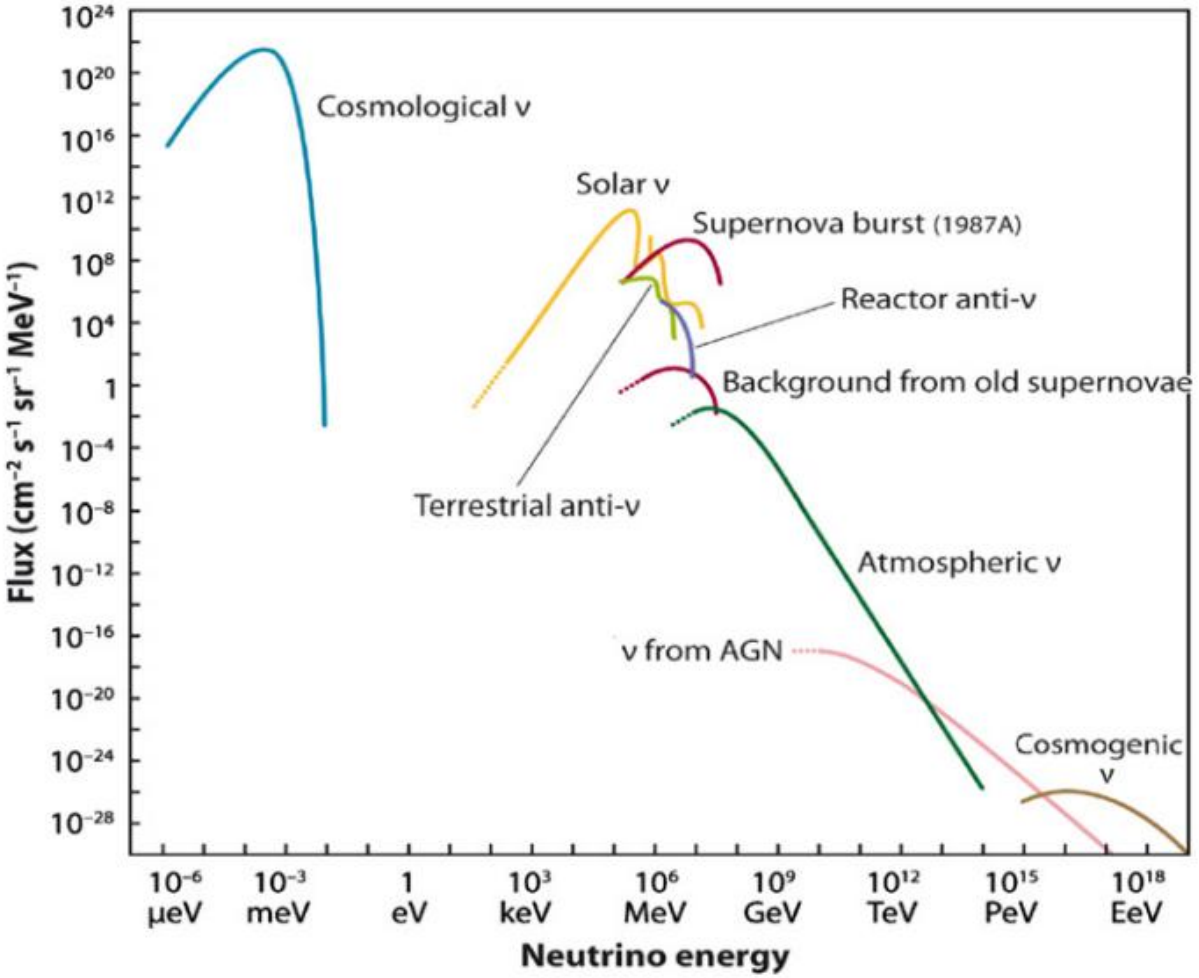

Fig. 1. Measured and expected fluxes of natural and reactor neutrinos.

High-energy neutrino astrophysics: Status and perspectives.
Progress in Particle and Nuclear Physics 67 (2012) 651–704

Flux Spectrum for Solar Neutrino

pp channel: $p + p \rightarrow d + e^+ + \nu_e$

pep channel: $p + e^- + p \rightarrow d + \nu_e$

hep channel: ${}^3He + p \rightarrow {}^4He + e^+ + \nu_e$

${}^7Be$ channel: ${}^7Be + e^- \rightarrow {}^7Li + \nu_e$

${}^8B$ channel: ${}^8B + e^- \rightarrow {}^8Be + \nu_e$

${}^{13}N$ channel: ${}^{13}N \rightarrow {}^{13}C + e^+ + \nu_e$

${}^{15}O$ channel: ${}^{15}O \rightarrow {}^{15}N + e^+ + \nu_e$

${}^{17}F$ channel: ${}^{17}F \rightarrow {}^{17}O + e^+ + \nu_e$

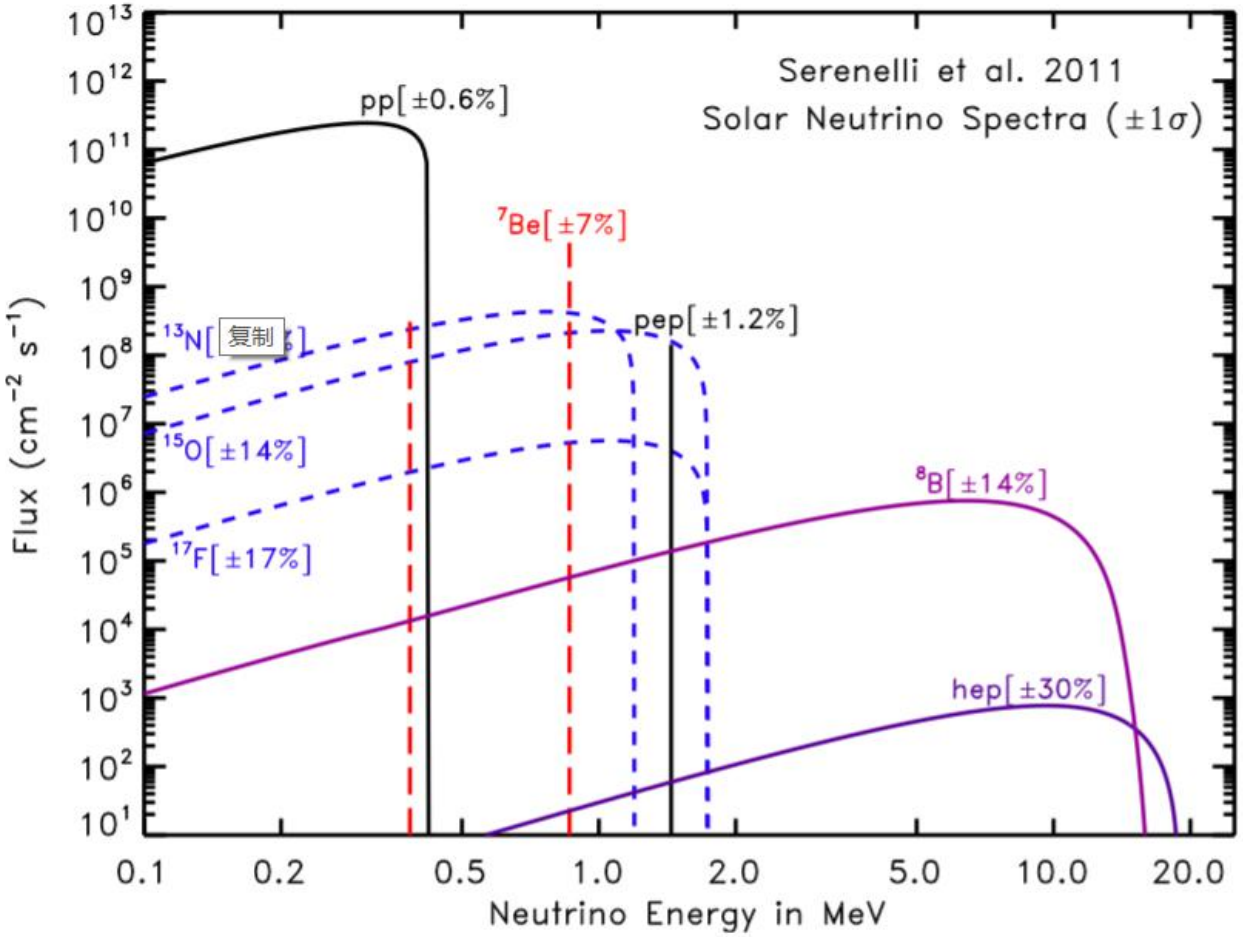

Solar Neutrinos: Status and Prospects, Annu. Rev. Astron. Astrophys. 51:21–61 2013

Millicharged Neutrino

Reaction Event Rate in Detectors

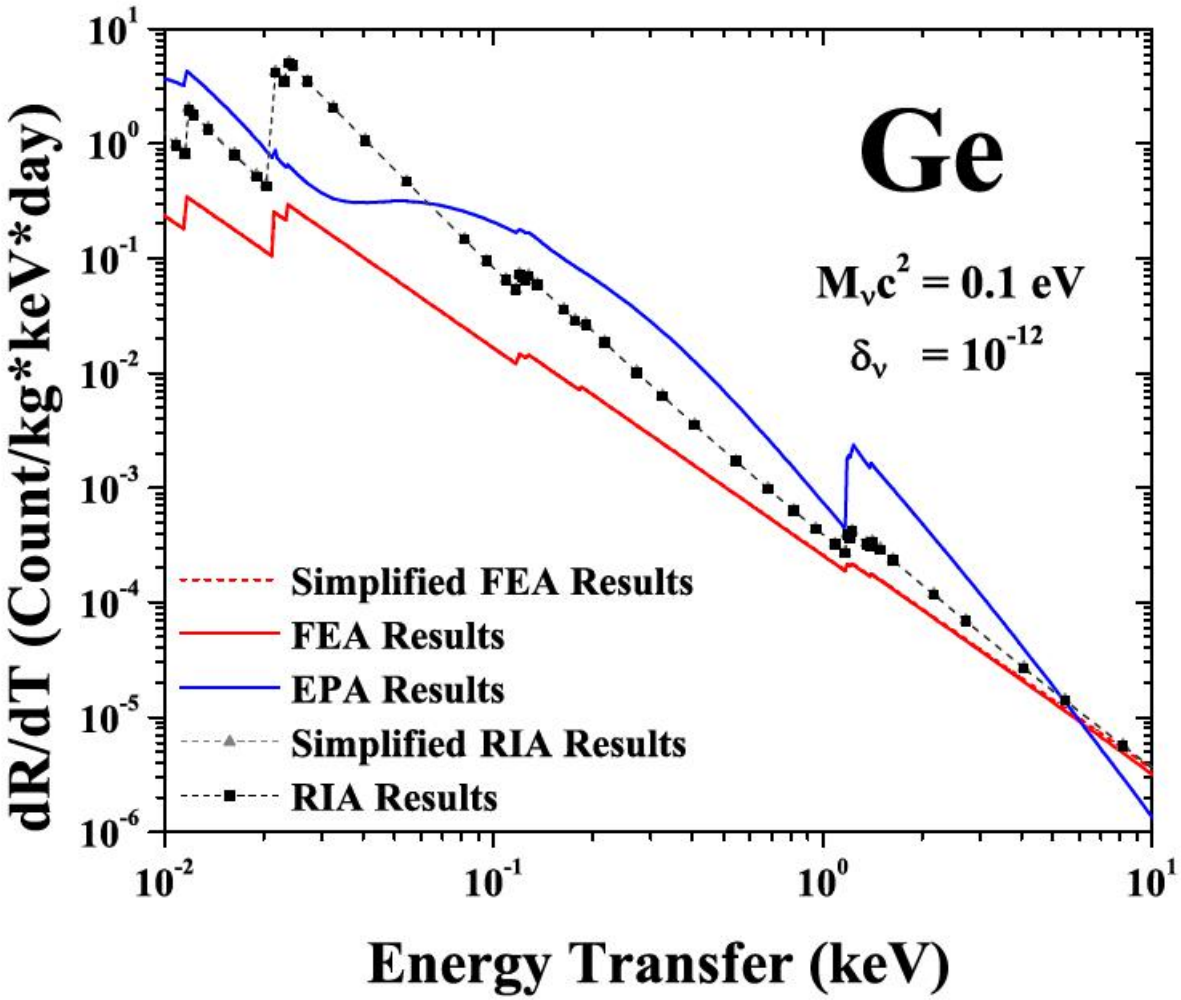

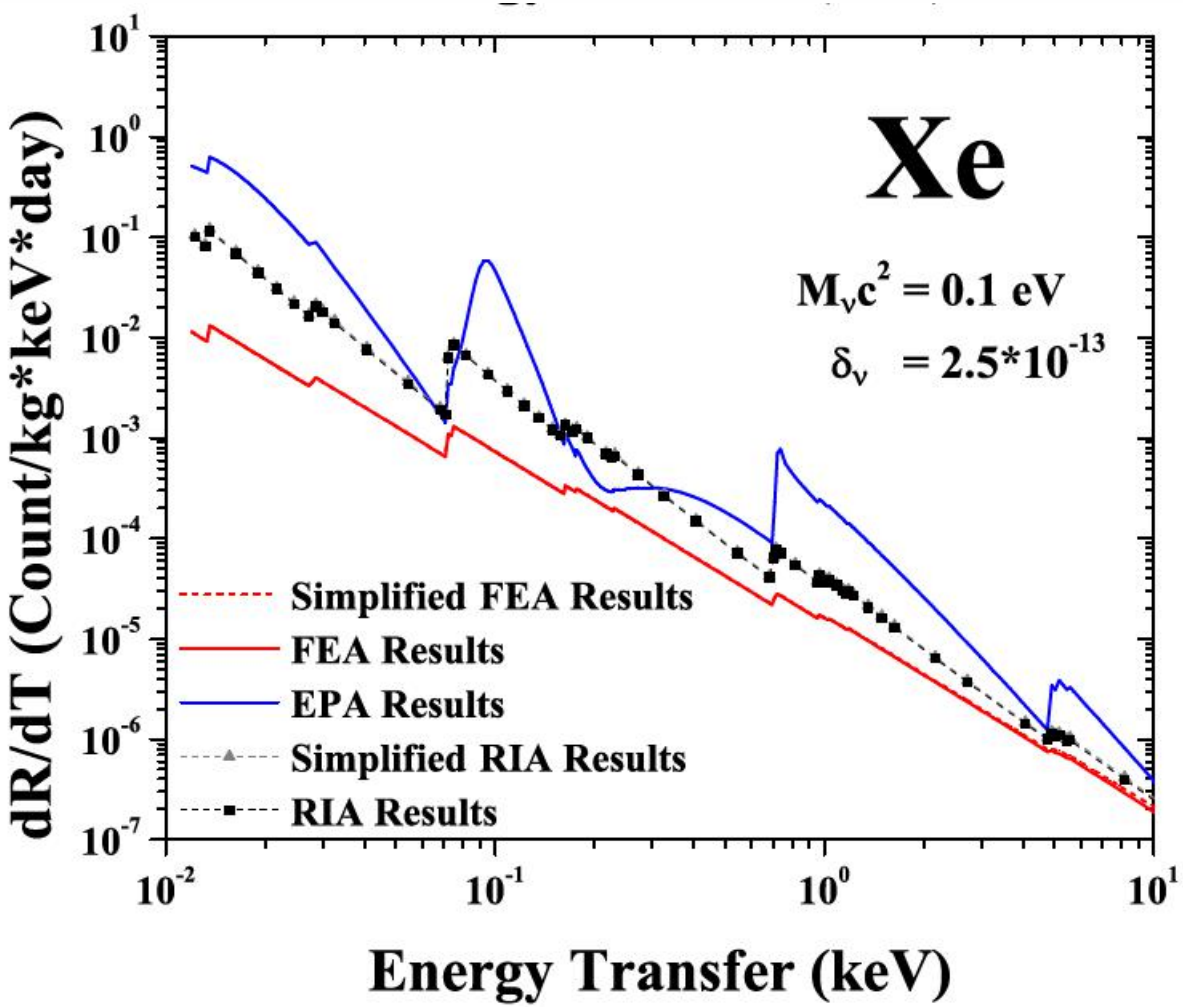

Experimental Constraint on Millicharged Neutrino

HPGe Detector	
Group	detecting sensitivity on neutrino millicharge δ_ν
Our Results	2.5×10^{-12} (FEA Results)
	7×10^{-13} (EPA Results)
	1×10^{-12} (RIA Results)
TEXONO [18]	2.1×10^{-12}
GEMMA [137]	1.5×10^{-12} / 2.7×10^{-12} (based on different methods)
LXe Detector	
Group	detecting sensitivity on neutrino millicharge δ_ν
Our Results	4×10^{-13} (FEA Results)
	9×10^{-14} (EPA Results)
	2.5×10^{-13} (RIA Results)
XENON1T [46]	6.4×10^{-13}
PandaX [138]	2.06×10^{-12}
Projected DARWIN [139]	2.4×10^{-13}
Projected LZ [140]	2.8×10^{-13}

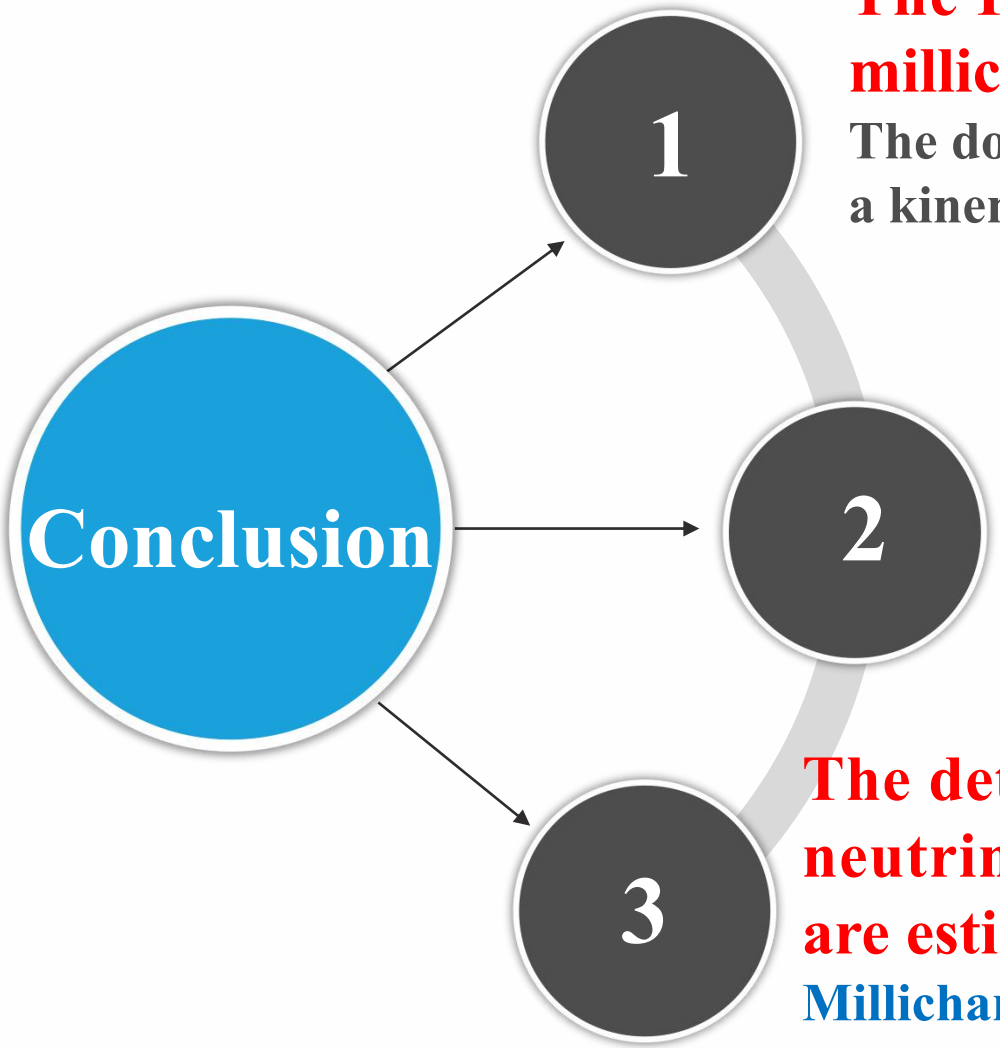

The RIA approach for atomic ionization induced by millicharged particle is derived.

The doubly-differential cross section is reduced to the product of a kinematical factor (Y) and Compton Profile (J) .

$$\left(\frac{d^2\sigma}{d\omega_f d\Omega_f}\right)_{\mathrm{RIA}} \propto J(p_z) \equiv \int \rho(\boldsymbol{p}) dp_x dp_y$$

The differential cross sections of atomic ionization induced process by MCP are calculated.

When energy transfer is sufficient large, RIA results and FEA results agree with each other.

The detecting sensitivities on dark matter particle and neutrino millicharge for next-generation experiments are estimated.

Millicharged dark matter particle:

2-3 orders of magnitude better than current experiments

Millicharged neutrino:

2-3 times better than current experiments

Prospects

Study Atomic Ionizations in Other Detectors

Liquid Ar Detector
NaI Detector
CsI Detector
.....

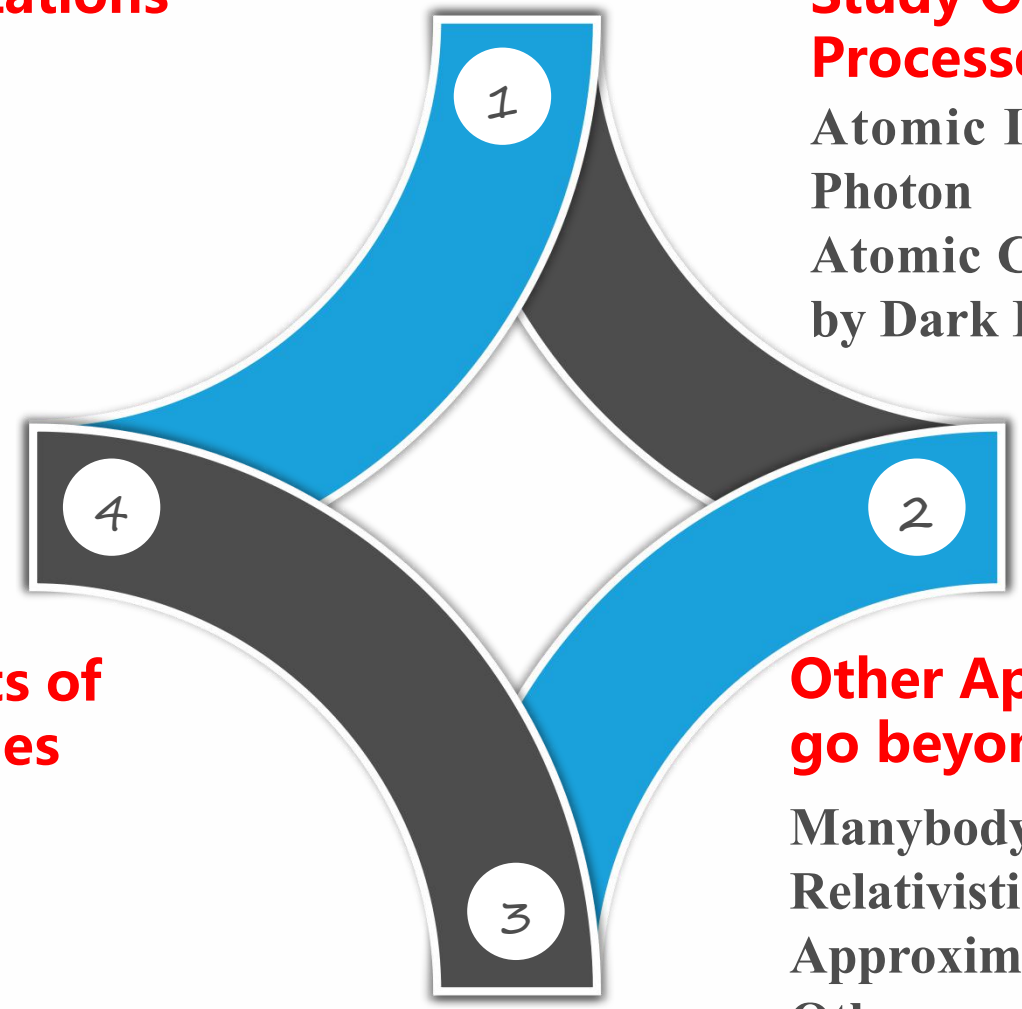

Study Other Electromagnetic Processed using RIA

Atomic Ionization induced by Dark Photon
Atomic Compton Scattering induced by Dark Photon

Study Other Aspects of Millicharged Particles

Charge Radius
Magnetic Moment
.....

Other Approaches which may go beyond RIA

Manybody QED
Relativistic Random-Phase Approximation (RRPA)
Other approach from Atomic, Molecular and Condensed matter physics

Thanks